Efficient signal reconstruction scheme for *M*-channel time-interleaved ADCs

Anu Kalidas Muralidharan Pillai and Håkan Johansson

The original publication is available at www.springerlink.com:

Anu Kalidas Muralidharan Pillai and Håkan Johansson, Efficient signal reconstruction scheme for *M*-channel time-interleaved ADCs, 2013, Analog Integrated Circuits and Signal Processing, (77), 2, 113-122.
http://dx.doi.org/10.1007/s10470-013-0115-x

Noname manuscript No.
(will be inserted by the editor)

Efficient Signal Reconstruction Scheme for M-Channel Time-Interleaved ADCs

Anu Kalidas Muralidharan Pillai · Håkan Johansson

Received: date / Accepted: date

Abstract In time-interleaved analog-to-digital converters (TI-ADCs), the timing mismatches between the channels result in a periodically nonuniformly sampled sequence at the output. Such nonuniformly sampled output limits the achievable resolution of the TI-ADC. In order to correct the errors due to timing mismatches, the output of the TI-ADC is passed through a digital time-varying finite-length impulse response (FIR) reconstructor. Such reconstructors convert the nonuniformly sampled output sequence to a uniformly spaced output. Since the reconstructor runs at the output rate of the TI-ADC, it is beneficial to reduce the number of coefficient multipliers in the reconstructor. Also, it is advantageous to have as few coefficient updates as possible when the timing errors change. Reconstructors that reduce the number of multipliers to be updated online do so at a cost of increased number of multiplications per corrected output sample. This paper proposes a technique which can be used to reduce the number of reconstructor coefficients that need to be updated online without increasing the number of multiplications per corrected output sample.

Keywords Finite-length impulse response (FIR) filters · least-squares design · two-rate approach · periodically nonuniform sampling · time-interleaved analog-to-digital converters (TI-ADCs) · reconstruction filters.

1 Introduction

High-speed analog-to-digital converters (ADCs) typically use time-interleaving of multiple ADCs to reduce the requirements on the individual ADCs [1, 2]. The performance of such a time-interleaved ADC (TI-ADC) depends to a major extent on how well the individual ADCs are matched. Mismatches in gain, offset, and timing affects the overall performance of the ADC [3, 4]. In an ideal TI-ADC, the relative time-skew between the channel clocks should be uniform so as to form uniformly spaced samples at the output of the TI-ADC as shown in Fig. 1(a). However, timing mismatches between the channels result in a nonuniformly sampled sequence at the output. Reducing the effect of these timing mismatches can be done either in the analog or in the digital domain. In this paper we focus on the digital correction of errors introduced due to timing mismatches between the channels. Digital signal processing techniques are applied on the output samples of the TI-ADC to digitally correct for the mismatch errors. At very high bandwidths, the channel mismatches are frequency dependent. Hence, to achieve very high resolutions at high sampling frequencies, the reconstructors should compensate for the mismatches in the frequency responses between the channels [5–8]. For applications with moderate bandwidth and resolution, the time-skew errors can be considered as frequency-independent. Here, we consider the digital correction of errors due to static timing mismatches in M-channel TI-ADCs. It should be noted that even though the emphasis here is on TI-ADCs, these techniques can be applied to other applications where reconstructors are used to convert periodically nonuniform samples to uniformly spaced samples [9].

In a TI-ADC, static time-skew errors will result in a periodically nonuniformly sampled sequence as shown in Fig. 1(b). Several techniques have been proposed to reconstruct such bandlimited nonuniformly sampled signals [5, 10–18]. The complexity of such reconstructors are usually measured in terms of the number and the type of multipliers used to implement the reconstructor. For example, variable-coefficient multipliers are required if the coefficients of the

Anu Kalidas Muralidharan Pillai · Håkan Johansson
Division of Electronics Systems
Department of Electrical Engineering
Linköping University
Linköping, SE-581 83, Sweden
E-mail: kalidas@isy.liu.se, hakanj@isy.liu.se

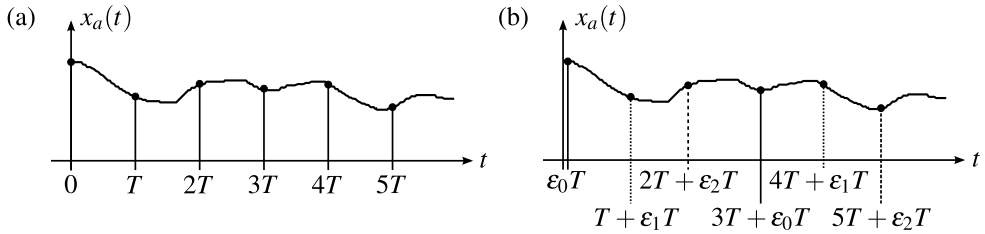

Fig. 1 (a) Uniformly sampled sequence. (b) Periodic nonuniform sampling ($M = 3$).

reconstructor need redesign whenever the time-skew errors change. Also, to implement the online redesign block, additional circuitry will be required which results in increased area and power consumption. Even though the power consumption of the online redesign block can be neglected if the redesign rate is much lower than the rate at which the reconstructor runs, the operation of the online redesign block may be time-critical. So it is still important to have a simpler online redesign block. Compared to the redesign block, the reconstructor always runs at the output rate of the TI-ADC. Hence, a rough measure of the reconstructor power consumption is the number of multipliers, adders, and delay elements that it contains. Since the number of adders scale proportionally with the number of multipliers, for complexity comparison, we consider only the number of multipliers and delay elements.

At one end of the complexity spectrum is the regular reconstructor [13] which uses a time-varying finite-length impulse response (FIR) structure to reconstruct M-periodic nonuniformly sampled signals. The regular reconstructor has the minimum order and requires the minimum number of delay elements. Since all the coefficients of the regular reconstructor need online redesign when the time-skew errors change, all the multipliers are implemented using expensive variable-coefficient multipliers. However, the regular reconstructor has the least number of multiplications per corrected output sample[1]. On the other end of the complexity spectrum is the reconstructor in [16] which does not require any online redesign. The iterative M-channel reconstructor in [16] uses differentiator-multiplier cascade (DMC) or DMC with reduced delay (DMC-RD) structures. In general, for a given M-channel specification, the DMC reconstructor requires the least number of fixed and variable-coefficient multipliers. However, due to a cascaded structure which does not allow sharing of delay elements, the DMC reconstructor requires more delay elements and larger group delay compared to the regular reconstructor. The DMC reconstructor also requires more multiplier operations per corrected output sample compared to the regular reconstructor.

[1] It is noted that, since each of the $M-1$ channels of a TI-ADC needs reconstruction, the complexity in terms of the total number of multipliers increases with M. However, the number of multiplications per corrected output sample is essentially independent of M.

The two-rate based (TRB) reconstructors [14, 19] have complexities in-between those of the regular and the DMC reconstructor. The TRB approach splits the reconstructor into two subfilters. All the coefficients in one of the subfilters are fixed and are implemented using less expensive fixed-coefficient multipliers. The coefficients of the second subfilter need to be redesigned online whenever the time-skew errors change. However, compared to the regular reconstructor, the second subfilter has fewer coefficients resulting in a simpler online redesign block. Compared to the DMC reconstructor, the TRB reconstructors require fewer multiplications per corrected output sample and fewer delay elements. While the TRB reconstructor design methods in [14, 19] are applicable only for the two-periodic case, the TRB multivariate impulse response (TRB-MIR) reconstructor in [17] can be used for the reconstruction of any M-periodic nonuniformly sampled sequence. Even though the TRB-MIR reconstructor do not require online redesign and needs fewer delay elements compared to the DMC reconstructor, the structure is attractive only for relatively smaller values of time-skew errors. The reconstructor in [5] uses the Gauss-Seidel iteration (GSI) method to derive an efficient iteration-based reconstructor that achieves faster convergence compared to other iteration-based reconstructors like the DMC reconstructor or the one in [7]. However, as [5] uses a recursive structure, the comparison with non-recursive structures is non-trivial as the effects of maximal sample-rate limitations [20] and numerical stability issues [21] need to be considered. Hence, [5] is not used here for comparison.

In this paper, we extend the two-periodic TRB reconstructor [19], to reconstruct any M-periodic nonuniformly sampled signal. Here we deal with the correction of the time-skew error and assume that the time-skew errors are estimated and available beforehand. Efficient correction schemes are desirable, for example, where reconstruction is performed by minimizing an appropriate cost measure using simultaneous estimation and correction [22]. Immediately following this introduction, a brief background on nonuniform sampling and reconstruction is provided in Section 2. In Section 3, the structure and design methodology for the M-periodic TRB reconstructor are outlined. Section 4 uses design examples to illustrate the savings obtained using the proposed structure. Section 5 concludes the paper.

2 Background

Uniform sampling of a continuous-time signal $x_a(t)$ at sampling instants $t = nT$ results in a discrete-time sequence $x(n)$ given by

$$x(n) = x_a(nT). \tag{1}$$

A nonuniformly sampled sequence, $v(n)$, is obtained if the sampling instants of $x_a(t)$ are $t = nT + \varepsilon_n T$. Hence,

$$v(n) = x_a(nT + \varepsilon_n T) \tag{2}$$

where ε_n is the percentage deviation (time-skew error) of the nth sample from the desired sampling instant nT. In an M-channel TI-ADC where the output samples are formed by interleaving the outputs from the individual subADCs, the time-skew error is M-periodic such that

$$\varepsilon_n = \varepsilon_{n+M}. \tag{3}$$

The output of such a TI-ADC will be an M-periodic nonuniformly sampled sequence. Figure 1(b) shows the periodically nonuniformly sampled sequence at the output of a three-channel TI-ADC. In order to simplify the design and implementation of the reconstructor, one of the TI-ADC channels is considered to be the reference channel. The time-skew errors of all the remaining channels are then expressed relative to the reference channel. Without loss of generality, here it is assumed that the zeroth channel is the reference channel. Also, we are interested in correcting the relative time skew between the channels. Hence, it suffices to assume that $\varepsilon_0 = 0$, ε_1 is the time-skew error between the first and the zeroth channel, ε_2 is the time-skew error between the second and the zeroth channel, and so on.

In order to recover the uniformly sampled sequence $x(n)$ from the nonuniformly sampled output $v(n)$, a time-varying discrete-time FIR reconstructor, $h_n(k)$, is used. To simplify derivations, $h_n(k)$ is assumed to be noncausal and of even order in all the equations. The reconstructor thus designed can be easily converted to its causal counterpart by adding suitable delays. By applying minor modifications to the indices, the same design methodology can be used to design odd-order reconstructors. The output of the reconstructor, $y(n)$, is given by

$$y(n) = \sum_{k=-N}^{N} v(n-k)h_n(k). \tag{4}$$

Assuming that $x_a(t)$ is bandlimited to ω_0 such that

$$X_a(j\omega) = 0, \;\; 0 < \omega_0 < |\omega|, \omega_0 < \frac{\pi}{T}, \tag{5}$$

it can be shown that the Fourier transforms of $x(n)$ and $x_a(t)$ are related as [13]

$$X(e^{j\omega T}) = \frac{1}{T} X_a(j\omega), \;\; -\pi \leq \omega T \leq \pi. \tag{6}$$

Representing $v(n-k)$ in terms of its inverse Fourier transform and using (2) and (6), it can be shown that (4) can be rewritten as [13]

$$y(n) = \frac{1}{2\pi} \int_{-\omega_0 T}^{\omega_0 T} A_n(j\omega T) X(e^{j\omega T}) e^{j\omega T n} d(\omega T) \tag{7}$$

where

$$A_n(j\omega T) = \sum_{k=-N}^{N} h_n(k) e^{-j\omega T(k-\varepsilon_{n-k})}. \tag{8}$$

For perfect reconstruction,

$$A_n(j\omega T) = 1, \;\; \omega T \in [-\omega_0 T, \omega_0 T] \tag{9}$$

so that the right-hand side of (7) will be equal to the inverse Fourier transform of $x(n)$. Hence, by suitably selecting $h_n(k)$ such that (9) is satisfied, it is theoretically possible to reconstruct $x(n)$ from $y(n)$. However, since the impulse response of the reconstructor $h_n(k)$ is of finite length, it is not practically feasible to make $A_n(j\omega T)$ exactly equal to unity. In practice, the coefficients of $h_n(k)$ are determined such that, in the band of interest, $A_n(j\omega T)$ approximates unity with a certain error margin [13]. For a nonuniformly sampled sequence $y(n)$ with a periodically varying time-skew error as given in (3), the impulse response of the time-varying reconstructor in Fig. 2(a) will also be periodic such that

$$h_n(k) = h_{n+M}(k). \tag{10}$$

Using multirate theory [23] and (10), the reconstructor in Fig. 2(a) can be represented as an M-channel maximally decimated filter-bank (FB) as shown in Fig. 2(b)[2]. Since the time-skew error of the reference channel (assumed here to be the first channel) is zero, the samples from the first channel will be passed directly to the output without any correction. Hence, in Fig. 2(b), $H_0(z) = 1$ which corresponds to $h_0(k) = \delta(k)$. So the reconstructor design for an M-channel TI-ADC involves designing the coefficients of $h_n(k)$ for $n = 1, 2, \ldots, M-1$ such that, for a given bandwidth $\omega_0 T$, the error between $A_n(j\omega T)$ and unity is minimized in some sense. The least-squares based reconstructor design approach [13] involves minimizing an error power function

$$P_n = \frac{1}{2\pi} \int_{-\omega_0 T}^{\omega_0 T} |A_n(j\omega T) - 1|^2 d(\omega T). \tag{11}$$

The time-skew errors in a TI-ADC can change over a period of time, for example, due to temperature variations. The magnitude of these time-skew errors do not change from sample to sample, but rather between blocks of samples.

[2] The noncausal blocks, z^m, $m = 1, 2, \cdots, M-1$, are only used for convenience in representing the reconstructor. They will not be present in the actual implementation.

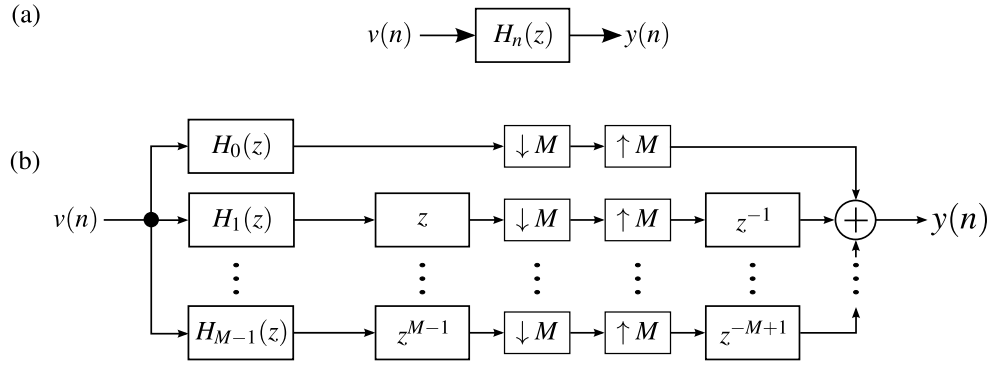

Fig. 2 (a) Time-varying FIR reconstructor. (b) Equivalent M-channel maximally decimated FB representation. Usually, in order to simplify the design and implementation of the reconstructor, it is assumed that $H_0(z) = 1$.

An approach for designing the reconstructors $H_n(z)$ in Fig. 2(b) was introduced in [13]. With this approach, all the coefficients of $h_n(k)$ had to be redesigned when ε_n changes. In [13], (11) is used to derive a closed-form solution for the least-squares minimization problem which can then be implemented online using matrix inversion. Since the online redesign block use matrix inversion, as the number of reconstructor coefficients to be redesigned increases so does the complexity of the online redesign block. For example, in the online redesign of a reconstructor of order $2N$, for each $h_n(k)$ where $n = 1, 2, \cdots, M-1$, a $(2N+1)\times(2N+1)$ matrix should be inverted which has an implementation complexity of $O(N^3)$.

3 M-channel Two-Rate Based Reconstructors

The TRB reconstructor, which extends the basic two-rate approach [24, 25], helps to reduce the implementation complexity by splitting the regular reconstructor $H_n(z)$ in Fig. 2(b) into two subfilters namely $F(z)$ and $G^{(n)}(z)$ as shown in Fig. 3(a). The subfilter $F(z)$ is designed such that the coefficients of this filter can be used for all combinations of time-skew errors $\varepsilon_n \in [-\varepsilon_{max}, \varepsilon_{max}]$. The coefficients of the subfilter $G^{(n)}(z)$ is redesigned online whenever ε_n change.

The subfilter $F(z)$ is a linear-phase half-band filter [26] whose every odd impulse response coefficient is equal to zero. Using multirate theory [23], the TRB structure in Fig. 3(a) can be converted into an equivalent single-rate structure shown in Fig. 3(b). Here, $F_0(z)$, $F_1(z)$ and $G_0^{(n)}(z)$, $G_1^{(n)}(z)$ are the Type-I polyphase components [23] of $F(z)$ and $G^{(n)}(z)$, respectively, such that

$$f_0(k) = f(2k), \tag{12}$$

$$f_1(k) = f(2k+1), \tag{13}$$

and

$$g_0^{(n)}(k) = g^{(n)}(2k), \tag{14}$$

$$g_1^{(n)}(k) = g^{(n)}(2k+1). \tag{15}$$

Since $F_0(z)$ is the zeroth polyphase component of a linear-phase half-band filter, its impulse response coefficients are symmetric whereas $F_1(z)$, which is the first polyphase component of $F(z)$, is a pure delay equal to $z^{-(D_F-1)/2}$ with D_F being the delay of $F^{(n)}(z)$. As shown in Fig. 4, the reconstructor can be designed such that a single $F_0(z)$ can be shared among all the channels resulting in fewer fixed-coefficient multipliers. Here, D_G is the delay of $G(z)$. The delay z^{-1} in Fig. 3(b) is propagated into $F_1(z)$ to get

$$F_1(z) = z^{-(D_F+1)/2}. \tag{16}$$

Hence, the impulse response of the nth reconstructor $h_n(k)$ can be expressed as

$$h_n(k) = f_0(k) * g_0^{(n)}(k) + f_1(k) * g_1^{(n)}(k). \tag{17}$$

In Fig. 4, the multipliers in all the subfilters operate at the input rate. Figure 5 shows a lower-rate implementation of the TRB reconstructor for an M-channel TI-ADC. The structure in Fig. 5 is obtained by polyphase decomposing the subfilters $G_0^{(n)}(z)$ and $G_1^{(n)}(z)$ for $n = 1, 2, \ldots, M-1$, and by propagating the downsample by M into each branch. Since polyphase decomposition splits the multipliers in the subfilters among the M polyphase components, each polyphase component, $G_{rp}^{(n)}(z)$, will have only a few multipliers. The multipliers in the subfilter $F_0(z)$ operate at the input rate whereas all the multipliers in subfilters $G_{rp}^{(n)}(z)$, $n = 1, 2, \ldots, M-1$, $r = 0, 1$, $p = 0, 1, 2, \ldots, M-1$ operate at $1/M$th of the input rate.

The design of the M-channel reconstructor in Fig. 4 involves determining the coefficients of the subfilters $F_0(z)$, $G_0^{(n)}(z)$, and $G_1^{(n)}(z)$ for $n = 1, 2, \ldots, M-1$. The design is split into two steps namely the offline design of $F_0(z)$ and the online redesign of $G_0^{(n)}(z)$ and $G_1^{(n)}(z)$ whenever the time-skew errors change.

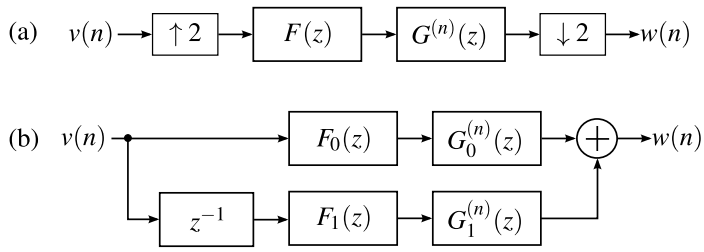

Fig. 3 (a) Equivalent two-rate representation of $H_m(z)$. (b) Single-rate realization of (a) using Type-I polyphase components of $F^{(n)}(z)$ and $G^{(n)}(z)$.

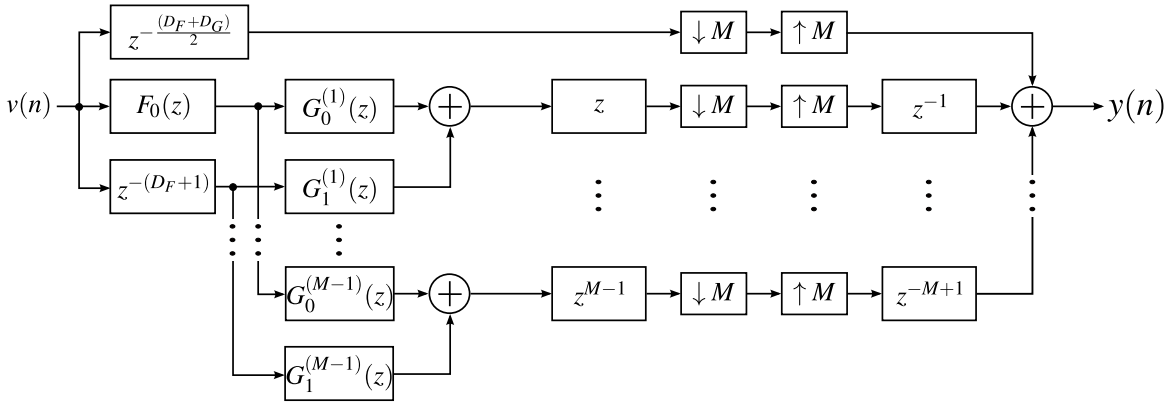

Fig. 4 Maximally decimated FB representation of an M-channel TRB reconstructor.

3.1 Offline design of $F_0(z)$

A least-squares approach is used to design $F_0(z)$ and the design problem is formulated as:

Given the orders of the subfilters $F_0(z)$, $G_0^{(0)}(z)$, and $G_1^{(0)}(z)$ as well as all the possible combinations of M time-skew errors ε_n, $n = 0,\ 1,\ \ldots,\ M-1$ where each ε_n can take either $-\varepsilon_{max}$ or ε_{max}, determine the coefficients of these subfilters and a parameter δ, to minimize δ subject to

$$\frac{1}{2\pi}\int_{-\omega_0 T}^{\omega_0 T} |A_0(j\omega T)-1|^2 d(\omega T) \le \delta. \tag{18}$$

Usually, the requirement on the maximal reconstruction error, δ_e, is satisfied if, after optimization, $\delta \le \delta_e$. It should be noted that in the above problem formulation, the subfilters are designed assuming that also the time-skew error of the reference channel (corresponding to $n = 0$) is either $-\varepsilon_{max}$ or ε_{max}. This is required in the offline design step, since the coefficients of $F_0(z)$ are determined in such a way that (18) holds for channel zero for all the possible combinations of $\varepsilon_n \in [-\varepsilon_{max}, \varepsilon_{max}]$. However, in the reconstructor implementation, the time-skew error of the reference channel is assumed to be equal to zero. Since the TRB reconstructor consists of a cascade of subfilters, the optimization problem in (18) is nonlinear in nature. Hence, to avoid a poor local optimum, a good starting point is used for the coefficients of the subfilters. The following steps summarize the design procedure to avoid a poor local optimum.

1. Compute the order, $\widetilde{N}_F$, of a standard half-band linear-phase FIR filter $F(z)$ whose passband and stopband edges are $\Omega_c = \omega_0 T/2$ and $\Omega_s = \pi - \Omega_c$, respectively, and with $\sqrt{\delta_e}$ as the maximum ripple in the passband and stopband[3].
2. Compute the order, $\widetilde{N}_G$, of a filter $G^{(0)}(z)$ such that it approximates a regular reconstruction filter [13] with δ_e as the magnitude of the reconstruction error and bandwidth Ω_c.
3. For each combination of N_F and N_G around the values of $\widetilde{N}_F$ and $\widetilde{N}_G$:
   (a) Design a regular half-band filter, $F(z)$, whose passband and stopband edges are at $\Omega_c = \omega_0 T/2$ and $\Omega_s = \pi - \Omega_c$, respectively, and with $\sqrt{\delta_e}$ as the maximum ripple in the passband and stopband. Use polyphase decomposition to split the $F(z)$ filter into $F_0(z)$ and a pure delay term $z^{-(D_F+1)/2}$.
   (b) Design a regular reconstructor $G^{(0)}(z)$ with reconstruction error δ_e and bandwidth Ω_c. Obtain the coefficients for $G_0^{(0)}(z)$ and $G_1^{(0)}(z)$ using polyphase decomposition.
   (c) Determine the subfilter coefficients by solving the optimization problem in (18) by using the coefficients for $F_0(z)$, $G_0^{(0)}(z)$, and $G_1^{(0)}(z)$, determined in Steps 3(a) and 3(b), as the initial values for the optimization. Save the subfilter coefficients if the δ obtained

[3] We use $\sqrt{\delta_e}$ since the error power in (18) is a square of the error magnitude.

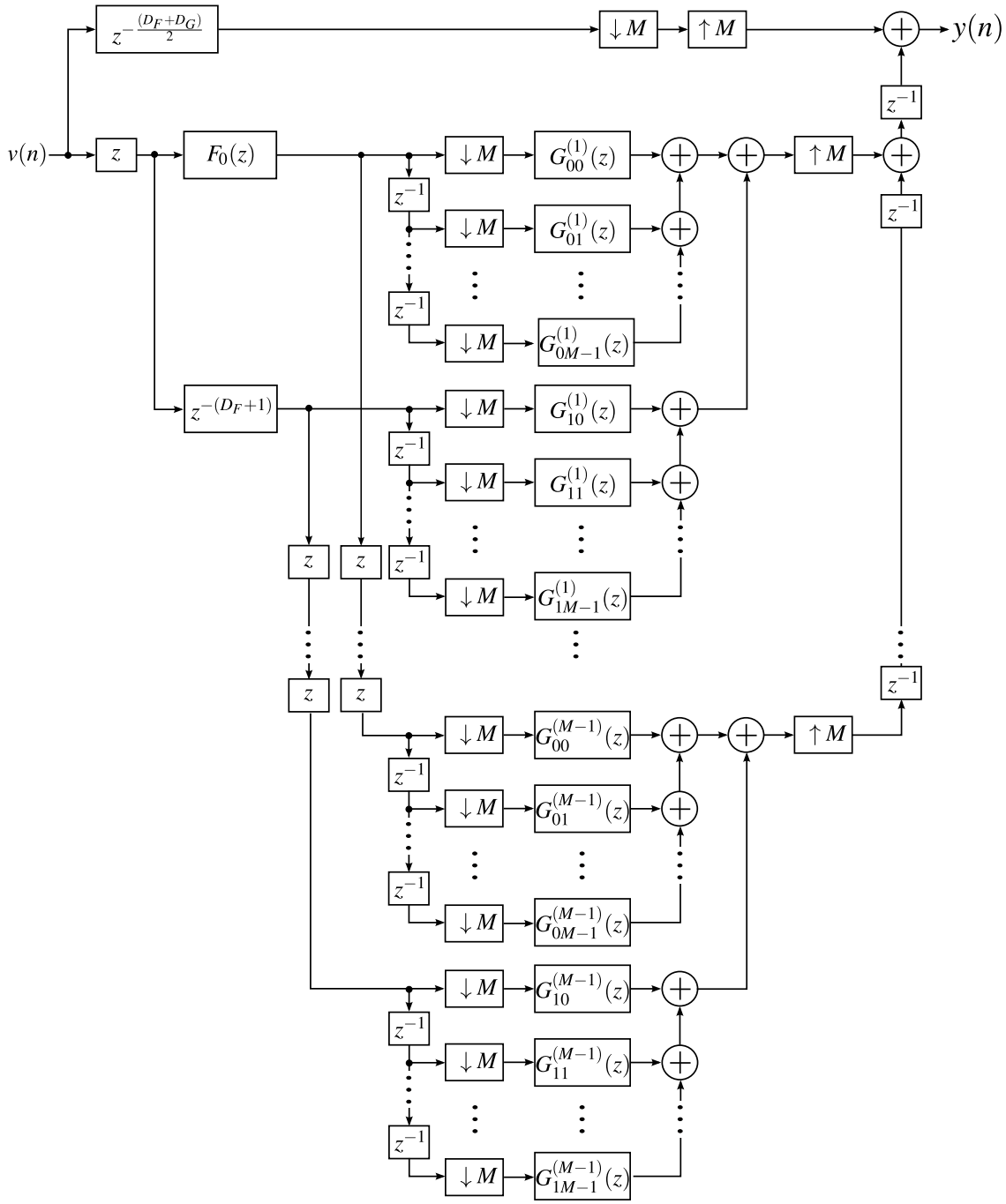

Fig. 5 Lower-rate implementation of the TRB reconstructor for an M-channel TI-ADC. Multipliers in $F_0(z)$ operate at the input rate whereas the multipliers in subfilters $G_{rp}^{(n)}(z)$ operate at $1/M$th the input rate.

after the optimization routine is smaller than the specified δ_e.

4. From all the saved results in Step 3(c), select the one with the least N_G as the final solution in order to minimize the complexity of online design of $G_0^{(n)}(z)$ and $G_1^{(n)}(z)$ for $n = 1, 2, \ldots, M-1$.

The subfilter $F_0(z)$, designed using the above steps, can be used for all $\varepsilon_n \in [-\varepsilon_{max}, \varepsilon_{max}]$. As the magnitude of the time-skew errors reduce, the sampling pattern becomes less nonuniform and a lower-order reconstructor can be used to achieve the same reconstruction error [13]. Therefore, when the time-skew error starts to decrease from the extremes $\pm\varepsilon_{max}$ and approaches 0, the reconstruction system becomes simpler. Hence, only the coefficients of the subfilters $G_0^{(n)}(z)$ and $G_1^{(n)}(z)$, $n = 1, 2, \ldots, M-1$ need to be determined for the new time-skew error.

3.2 Online design of $G_0^{(n)}(z)$ and $G_1^{(n)}(z)$

Using a least-squares approach for the design of the subfilters $G_0^{(n)}(z)$ and $G_1^{(n)}(z)$ allows us to implement the online redesign block using matrix inversions.

If the order of $F(z)$ is assumed to be $4N_F+2$ (since $F(z)$ is a half-band filter), the length of the subfilter $F_0(z)$ will be $2N_F$. Hence, the impulse response of $F_0(z)$ is denoted as

$$\mathbf{f}_0 = [f_0(-N_F)\ \ f_0(-N_F+1)\ \ \ldots\ f_0(N_F-1)] \tag{19}$$

whereas the delay term $z^{-(D_F+1)/2}$ in Fig. 4 is a sequence of length $2N$ denoted by

$$\mathbf{f}_1 = [f_1(-N_F)\ \ f_1(-N_F+1)\ \ \ldots\ f_1(N_F-1)] \tag{20}$$

with

$$f_1(k) = \begin{cases} 1, & k=1 \\ 0, & k\neq 1 \end{cases}. \tag{21}$$

If $\mathbf{g}_0^{(n)}$ and $\mathbf{g}_1^{(n)}$ are the impulse response vectors of $G_0^{(n)}(z)$ and $G_1^{(n)}(z)$, respectively,

$$\mathbf{g}_0^{(n)} = [g_0^{(n)}(-N_G)\ \ g_0^{(n)}(-N_G+1)\ \ \ldots\ g_0^{(n)}(N_G)] \tag{22}$$

and

$$\mathbf{g}_1^{(n)} = [g_1^{(n)}(-N_G)\ \ g_1^{(n)}(-N_G+1)\ \ \ldots\ g_1^{(n)}(N_G)] \tag{23}$$

where both $\mathbf{g}_0^{(n)}$ and $\mathbf{g}_1^{(n)}$ are assumed to have a length of $2N_G+1$ to simplify the calculations. By adjusting the indices, the design can be easily modified for any combination of impulse response lengths for $\mathbf{g}_0^{(n)}$ and $\mathbf{g}_1^{(n)}$.

Now, (17) can be expressed as

$$\mathbf{h}_n = \mathbf{F}\mathbf{g}_n \tag{24}$$

where

$$\mathbf{F} = [\mathbf{F}_0^T\ \ \mathbf{F}_1^T] \tag{25}$$

and

$$\mathbf{g}_n = [\mathbf{g}_0^{(n)}\mathbf{g}_1^{(n)}]^T. \tag{26}$$

Also,

$$\mathbf{F}_0 = [\mathbf{F}_{t0}^T\ \ \mathbf{Z}_{2N_F+2N_G,2N_G+1}^T] \tag{27}$$

and

$$\mathbf{F}_1 = [\mathbf{Z}_{2N_F+2N_G,2N_G+1}^T\ \ \mathbf{F}_{t1}^T] \tag{28}$$

where $\mathbf{Z}_{r,q}$ is an $r\times q$ zero matrix and $\mathbf{F}_{tr}$ is a $(2N_F+2N_G)\times(2N_G+1)$ Toeplitz matrix with first row $[f_r(-N_F)\ \ \mathbf{Z}_{1,2N_G}]$ and first column $[\mathbf{f}_r\ \ \mathbf{Z}_{1,2N_G}]^T$.

Using (24) to express (8) in matrix form and substituting the result in (11) followed by some algebraic manipulations, we get

$$P_n = \mathbf{g}_n^T\mathbf{F}^T\mathbf{S}_n\mathbf{F}\mathbf{g}_n + \mathbf{g}_n^T\mathbf{F}^T\mathbf{b}_n + C \tag{29}$$

where

$$\mathbf{S}_n = [\widetilde{\mathbf{S}}_{n,kp}^T\ \ \widetilde{\mathbf{S}}_{n,kp}^T]^T, \tag{30}$$

$$\widetilde{\mathbf{S}}_{n,kp} = \begin{cases} \frac{\omega_0 T}{\pi}, & p=k \\ \frac{\sin(\omega_0 T(p-k-\varepsilon_{n-p}+\varepsilon_{n-k}))}{\pi(p-k-\varepsilon_{n-p}+\varepsilon_{n-k})}, & p\neq k \end{cases}, \tag{31}$$

$$\mathbf{b}_n = \begin{cases} -\frac{2\omega_0 T}{\pi}, & k=\varepsilon_{n-k} \\ -\frac{2\sin(\omega_0 T(k-\varepsilon_{n-k}))}{\pi(k-\varepsilon_{n-k})}, & k\neq\varepsilon_{n-k} \end{cases}, \tag{32}$$

and

$$C = \frac{\omega_0 T}{\pi} \tag{33}$$

with $p,k=-R,\ -R+1,\ \ldots R-1$ and $2R=2N_F+2N_G$ is the length of $h_n(k)$. Solving

$$\frac{\partial P_n}{\partial \mathbf{g}_n} = 0 \tag{34}$$

gives the value of $\mathbf{g}_n$ that minimizes the error power function P_n. Substituting (29) in (34) gives

$$\mathbf{g}_n = -0.5(\mathbf{F}^T\mathbf{S}_n\mathbf{F})^{-1}\mathbf{F}^T\mathbf{b}_n. \tag{35}$$

From (35), it can be seen that, the online design of $G_0^{(n)}(z)$ and $G_1^{(n)}(z)$, $n=1,\ 2,\ \ldots,\ M-1$, require $M-1$ separate matrix inversions[4].

4 Design Example

In this example, we consider the design of a reconstructor for a four-channel TI-ADC with the following specification: $\omega_0 T = 0.8\pi$, $\varepsilon_{max}\in[-0.02, 0.02]$, and a maximum reconstruction error of $P_n \approx 80$ dB. This specification is the same as that considered in [13], [16], and [17]. Thus, we can compare the complexity of the four reconstructors since all the reconstructors are designed to meet the same specification. Following the design steps in Section 3.1, the coefficients of the subfilter $F_0(z)$ are determined so that they can be used for any value of time-skew error, $\varepsilon_n\in[-0.02, 0.02]$. The number of coefficients in the subfilter $F_0(z)$, which resulted in minimum complexity of the variable-coefficient subfilter, turned out to be 8. For this $F_0(z)$, the length of $G_0^{(n)}(z)$ and

[4] In TI-ADC implementations, the typical values of time-skew errors is less than 10%. For values of time-skew errors in this range, the matrix to be inverted in (35) is not ill-conditioned. However, it should also be possible to use other online methods such as the RLS algorithm for the design of $G_0^{(n)}(z)$ and $G_1^{(n)}(z)$.

$G_1^{(n)}(z)$ turned out to be 4 and 3, respectively. Hence, the above reconstructor requires 8 fixed-coefficient multipliers and 21 variable-coefficient multipliers. To meet the above specification, the regular reconstructor [13] would require 15 variable-coefficient multipliers in each of the three channels. In addition to an increase in the number of variable-coefficient multipliers, the online redesign block for each channel of the regular reconstructor will require inverting a 15×15 matrix whereas the online redesign for each channel of the proposed TRB reconstructor can be implemented with a 7×7 matrix inversion. For the above specification, the TRB-MIR reconstructor [17] requires 40 fixed-coefficient and 5 variable-coefficient multipliers. While the reconstructor in [17] needs no online redesign, it is noted that compared to the proposed method, the design method in [17] is applicable only for relatively smaller time-skew errors. The DMC reconstructor [16] that meets the specification in this example would require 33 fixed-coefficient multipliers, 3 variable-coefficient multipliers and no online redesign. However, the DMC reconstructor needs 66 delay elements whereas, using direct-form implementation, the proposed TRB reconstructor would require only 20 delay elements. Using the lower-rate implementation shown in Fig. 5, the fixed-coefficient multipliers operate at the input rate whereas the variable-coefficient multipliers operate at one-fourth the input rate. It should be noted that all the polyphase decomposed components, except $G_{13}^{(n)}(z)$, $n = 1,\ 2,\ 3$, will have 1 multiplier each whereas $G_{13}^{(n)}(z)$, $n = 1,\ 2,\ 3$ does not require any multiplier. The proposed reconstructor thus requires 15 multiplications to generate one corrected output sample which is the same as that required by the regular reconstructor [13]. At the same time, the DMC [16] and the TRB-MIR [17] reconstructors require, respectively, 36 and 45 multiplications per corrected output sample. Table 1 summarizes the reconstructor complexity when the above specification is implemented using the regular [13], DMC [16], TRB-MIR [17], and the proposed TRB reconstructor design approaches. Here, we assume that, all the channel reconstructors are implemented in parallel using separate general multipliers. This helps to avoid the need for extra memory which will be required to store the variable-coefficients if the same set of general multipliers were shared between the channel reconstructors. From Table 1, it can be seen that, even though the complexity of the online design block in the proposed TRB reconstructor is in-between that of the regular and the DMC reconstructor, the overall complexity of the reconstructor designed using the proposed method is less compared to the regular and the DMC reconstructors.

Figure 6 shows the reconstructor errors for the first, second, and third channel where the coefficients of $G_0^{(n)}(z)$ and $G_1^{(n)}(z)$ are designed using the online design method outlined in Section 3.2 when the channel time-skew errors are

Table 1 Complexity comparison for Example 1.

Design	Delay elements	Multipliers		Multiplications per corrected sample
		Fixed	*General*	
[13]	15	0	45	15
[16]	66	33	9	36
[17]	31	40	15	45
Proposed	20	8	21	15

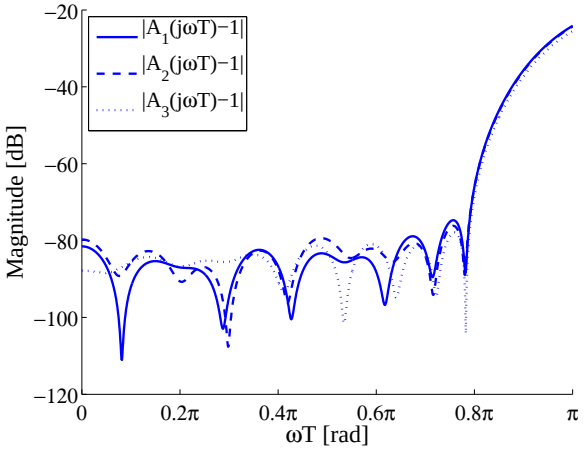

Fig. 6 Magnitude of $A_n(j\omega T) - 1$, $n = 1,\ 2,\ 3$, for the four-channel TRB reconstructor in Example 1, for $\varepsilon_0 = 0$, $\varepsilon_1 = -0.0195$, $\varepsilon_2 = 0.0194$, and $\varepsilon_3 = -0.0171$.

$\varepsilon_0 = 0$, $\varepsilon_1 = -0.0195$, $\varepsilon_2 = 0.0194$, and $\varepsilon_3 = -0.0171$. The above time-skew errors were randomly picked, within $\varepsilon_{max} \in [-0.02, 0.02]$, without any specific distribution function. Figure 7 shows the spectrum (normalized to 0 dB) of a nonuniformly sampled 16-bit multi-sine signal, $v(n)$, with the same channel time-skew errors as above. The spectrum of the reconstructed sequence, $y(n)$, is shown in Fig. 8. Figure 9 shows the histogram of the SNDR after reconstruction for uniformly distributed time-skew errors. For the histogram, we used a nonuniformly sampled sinusoidal signal whose frequency was increased in steps, from 0 to 0.8π, for each set of uniformly distributed time-skew errors. As can be seen from Fig. 9, the reconstructor is designed such that it gives an SNDR of at least 80 dB for the different combinations of time-skew errors.

5 Conclusion

This paper introduced a TRB reconstructor for correcting the effect of time-skew errors in an M-channel TI-ADC. With the help of design examples, it was shown that, compared to the regular reconstructor, the M-periodic TRB reconstructor offers savings in the total number of multipliers. The savings come at the cost of a slightly larger overall delay of the reconstructor. However, the TRB method sig-

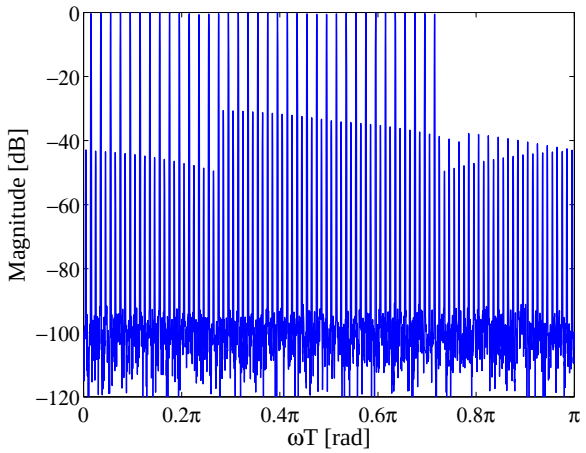

Fig. 7 Spectrum of the nonuniform sequence $v(n)$ in the design example.

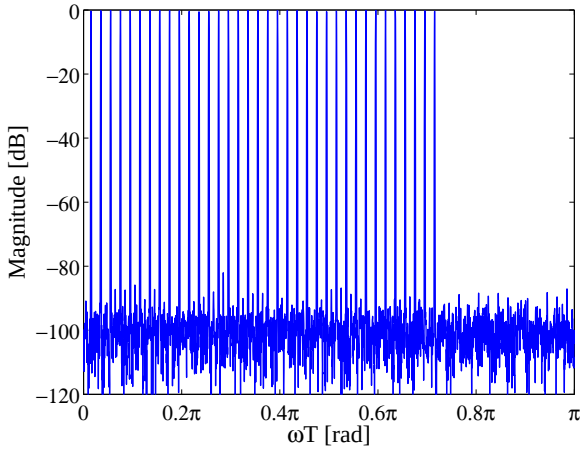

Fig. 8 Spectrum of the reconstructed sequence $y(n)$ in the design example.

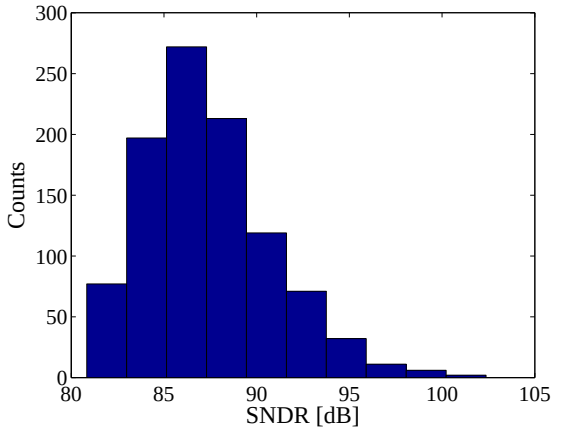

Fig. 9 Histogram of the SNDR after reconstruction in the design example with uniformly distributed time-skew errors.

nificantly reduces the number of reconstructor coefficients that need online redesign. This directly translates to lower complexity for the online redesign block. Compared to the regular reconstructor, the reduced complexity of the online redesign block as well as fewer multipliers help to reduce the overall area and power consumption. As outlined in the paper with the help of a design example, compared to the DMC reconstructor which do not need online redesign, the TRB reconstructor requires significantly fewer delay elements, lower group delay, and fewer multiplication per corrected output sample. The TRB reconstructor gives the designer an alternative where the online design complexities is in-between those of the regular and the DMC based reconstructor whereas the overall reconstructor complexity is lower compared to the regular and the DMC reconstructors.

References

1. W. C. Black and D. A. Hodges, "Time interleaved converter arrays," *IEEE J. Solid-State Circuits*, vol. 15, no. 6, pp. 1022–1029, Dec. 1980.
2. M. El-Chammas and B. Murmann, "A 12-GS/s 81-mW 5-bit time-interleaved flash ADC with background timing skew calibration," *IEEE J. Solid-State Circuits*, vol. 46, no. 4, pp. 838–847, Apr. 2011.
3. C. Vogel, "The impact of combined channel mismatch effects in time-interleaved ADCs," *IEEE Trans. Instrum. Meas.*, vol. 54, no. 1, pp. 415–427, 2005.
4. H. Kopmann and H. G. Göckler, "Error analysis of ultra-wideband hybrid analogue-to-digital conversion," in *Proc. XII European Sig. Proc. Conf. EUSIPCO*, Vienna, Austria, Sep. 6 –10 2004.
5. K. M. Tsui and S. C. Chan, "New iterative framework for frequency response mismatch correction in time-interleaved ADCs: Design and performance analysis," *IEEE Trans. Instrum. Meas.*, vol. 60, no. 12, pp. 3792–3805, Dec. 2011.
6. C. Vogel and S. Mendel, "A flexible and scalable structure to compensate frequency response mismatches in time-interleaved ADCs," *IEEE Trans. Circuits Syst. I*, vol. 56, no. 11, pp. 2463–2475, 2009.
7. H. Johansson, "A polynomial-based time-varying filter structure for the compensation of frequency-response mismatch errors in time-interleaved ADCs," *IEEE J. Sel. Topics Signal Process.*, vol. 3, no. 3, pp. 384–396, 2009.
8. S. Saleem and C. Vogel, "Adaptive blind background calibration of polynomial-represented frequency response mismatches in a two-channel time-interleaved ADC," *IEEE Trans. Circuits Syst. I*, vol. 58, no. 6, pp. 1300–1310, 2011.
9. F. Marvasti, Ed., *Nonuniform Sampling: Theory and Practice*. Kluwer Academic, Newyork, NY, USA, 2001.
10. J. Selva, "Functionally weighted lagrange interpolation of band-limited signals from nonuniform samples," *IEEE Trans. Signal Process.*, vol. 57, no. 1, pp. 168–181, Jan. 2009.
11. T. Strohmer and J. Tanner, "Fast reconstruction algorithms for periodic nonuniform sampling with applications to time-interleaved ADCs," in *Proc. IEEE Int. Conf. Acoustics, Speech and Signal Processing ICASSP 2007*, vol. 3, 2007.
12. E. Margolis and Y. C. Eldar, "Nonuniform sampling of periodic bandlimited signals," *IEEE Trans. Signal Process.*, vol. 56, no. 7, pp. 2728–2745, 2008.
13. H. Johansson and P. Löwenborg, "Reconstruction of nonuniformly sampled bandlimited signals by means of time-varying discrete-time FIR filters," *EURASIP J. Advances Signal Process.*, vol. 2006, Jan. 2006.

14. A. K. M. Pillai and H. Johansson, "Two-rate based low-complexity time-varying discrete-time FIR reconstructors for two-periodic nonuniformly sampled signals," *Sampling Theory in Signal and Image Processing - Special Issue on SampTA 2011*, accepted.
15. H. Johansson, P. Löwenborg, and K. Vengattaramane, "Least-squares and minimax design of polynomial impulse response FIR filters for reconstruction of two-periodic nonuniformly sampled signals," *IEEE Trans. Circuits Syst. I*, vol. 54, no. 4, pp. 877–888, Apr. 2007.
16. S. Tertinek and C. Vogel, "Reconstruction of nonuniformly sampled bandlimited signals using a differentiator–multiplier cascade," *IEEE Trans. Circuits Syst. I*, vol. 55, no. 8, pp. 2273–2286, Sep. 2008.
17. A. K. M. Pillai and H. Johansson, "Low-complexity two-rate based multivariate impulse response reconstructor for time-skew error correction in M-channel time-interleaved ADCs," in *Proc. IEEE Int. Symp. Circuits and Systems ISCAS*, May 2013.
18. H. Johansson, P. Löwenborg, and K. Vengattaramane, "Reconstruction of *M*-periodic nonuniformly sampled signals using multivariate impulse response time-varying FIR filters," in *Proc. XII Eur. Signal Process. Conf.*, Sep. 2006.
19. A. K. M. Pillai and H. Johansson, "Efficient signal reconstruction scheme for time-interleaved ADCs," in *Proc. IEEE 10th Int. New Circuits and Systems Conf. (NEWCAS)*, 2012, pp. 357–360.
20. M. Renfors and Y. Neuvo, "The maximum sampling rate of digital filters under hardware speed constraints," *IEEE Trans. Circuits Syst.*, vol. 28, no. 3, pp. 196–202, Mar. 1981.
21. A. Fettweis, "On assessing robustness of recursive digital filters," *Eur. Trans. Telecomm. Relat. Technol.*, vol. 1, no. 2, pp. 103–109, Mar.–Apr. 1990.
22. M. Seo, M. Rodwell, and U. Madhow, "Generalized blind mismatch correction for two-channel time-interleaved a-to-d converters," in *Proc. IEEE Int. Conf. Acoustics, Speech and Signal Processing ICASSP 2007*, vol. 3, 2007.
23. P. P. Vaidyanathan, *Multirate Systems and Filter Banks*. Prentice-Hall, Englewood Cliffs, NJ, USA, 1993.
24. N. P. Murphy, A. Krukowski, and I. Kale, "Implementation of wideband integer and fractional delay element," *Electronics Letters*, vol. 30, no. 20, pp. 1658–1659, 1994.
25. H. Johansson and E. Hermanowicz, "Two-rate based low-complexity variable fractional-delay FIR filter structures," *IEEE Trans. Circuits Syst. I: Regular Papers*, vol. 60, no. 1, pp. 136–149, Jan. 2013.
26. T. Saramäki, "Finite impulse response filter design," in *Handbook for Digital Signal Processing*, S. Mitra and J. Kaiser, Eds. Wiley, Newyork, 1993, ch. 4, pp. 155–277.